Published in final edited form as:
J Neural Eng. 2012 October ; 9(5): 056007. doi:10.1088/1741-2560/9/5/056007.

Signal distortion from microelectrodes in clinical EEG acquisition systems

William C. Stacey, MD PhD[1,2,*], **Spencer Kellis, PhD**[3], **Paras R. Patel, MSE**[2], **Bradley Greger, PhD**[4], and **Christopher R. Butson, PhD**[5]

[1]Department of Neurology, University of Michigan, Ann Arbor, MI

[2]Department of Biomedical Engineering, University of Michigan, Ann Arbor, MI

[3]Division of Biology, California Institute of Technology, Pasadena, CA

[4]Department of Bioengineering, University of Utah, SLC, UT

[5]Departments of Neurology and Neurosurgery, Medical College of Wisconsin, Milwaukee, WI

Abstract

Many centers are now using high-density microelectrodes during traditional intracranial EEG (iEEG) both for research and clinical purposes. These microelectrodes are FDA-approved and integrate into clinical EEG acquisition systems. However, the electrical characteristics of these electrodes are poorly described and clinical systems were not designed to use them; thus it is possible that this shift into clinical practice could have unintended consequences. In this study, we characterized the impedance of over 100 commercial macro- and microelectrodes using electrochemical impedance spectroscopy (EIS) to determine how electrode properties could affect signal acquisition and interpretation. The EIS data were combined with the published specifications of several commercial EEG systems to design digital filters that mimic the behavior of the electrodes and amplifiers. These filters were used to analyze simulated brain signals that contain a mixture of characteristic features commonly observed in iEEG. Each output was then processed with several common quantitative EEG measurements. Our results show that traditional macroelectrodes had low impedances and produced negligible distortion of the original signal. Brain tissue and electrical wiring also had negligible filtering effects. However, microelectrode impedances were much higher and more variable than the macroelectrodes. When connected to clinical amplifiers, higher impedance electrodes produced considerable distortion of the signal at low frequencies (< 60 Hz), which caused significant changes in amplitude, phase, variance, and spectral band power. In contrast, there were only minimal changes to the signal content for frequencies above 100 Hz. In order to minimize distortion with microelectrodes, we determined that an acquisition system should have an input impedance of at least 1 GΩ, which is much higher than most clinical systems. These results show that it is critical to account for variations in impedance when analyzing EEG from different-sized electrodes. Data from microelectrodes may yield misleading results unless recorded with high-impedance amplifiers.

Keywords

EEG; microelectrodes; electrodes; impedance; electrocorticography

[*]Address correspondence to: William Stacey MD PhD, University of Michigan, Department of Neurology, 1500 E. Medical Center Drive, SPC 5036, Ann Arbor, MI 48109-5036, USA, William.stacey@umich.edu, TEL: 734-936-7310, Fax: 734-936-5520 .

The authors have no conflict of interest to disclose.

INTRODUCTION

Intracranial electroencephalography (iEEG) is an invasive recording technique used when surface EEG cannot provide sufficient spatial resolution. This technology is used clinically for patients with epilepsy as well as in several other research endeavors such as electrocorticography (ECoG) for brain-machine interfaces (Ritaccio et al. 2010). These techniques have traditionally been conducted by sampling at 200 Hz or less using either subdural disc electrodes or intraparenchymal cylindrical depth electrodes, each with several square millimeters of conductive surface area. In recent years there has been great interest in recording with higher spatial and temporal resolution in order to improve understanding of network dynamics in both normal (Ritaccio et al. 2010) and pathological (Stacey et al. 2011a) brain networks.

Studies performed over the past decade have demonstrated that higher sampling rates can identify important clinical information in epilepsy (Worrell et al. 2004) and other disorders (Cimatti et al. 2007). These studies all rely upon higher temporal resolution, and their success has led to an increased demand for neurophysiological acquisition systems with higher sampling rates. Companies now offer clinical systems with upgraded acquisition hardware and anti-aliasing filters that are capable of sampling up to 1000-2000 Hz. Specialized systems are also available with much higher sampling rates.

Improved spatial resolution also holds great promise in iEEG. Clinical iEEG normally utilizes “macroelectrodes” that are usually disks about 4 mm diameter, spaced 1 cm apart. Recent research with much smaller “microelectrodes” has demonstrated brain activity such as high frequency oscillations (HFOs) (Le Van Quyen et al. 2010; Schevon et al. 2009; Worrell et al. 2008) and microseizures (Stead et al. 2010) that are not visible on the nearby macroelectrodes. These results have broad implications for research in epilepsy, cognition, and brain computer interfaces, which has led to an increasing demand for technology to conduct this research. In response, several electrode manufacturing companies now offer a selection of microelectrodes that can be placed between the macroelectrode contacts in clinical arrays, and have received FDA approval for clinical use in the United States. These integrated macro/microelectrode arrays are manufactured so that they can be connected to existing EEG acquisition hardware. Although this is clearly the most convenient method in clinical scenarios, most of the acquisition systems were designed to sample traditional iEEG: up to 128 macroelectrodes at 200 Hz sampling rate. For this reason, the research with microelectrodes mentioned above used specialized acquisition systems designed specifically for this type of data collection. Those specialized systems can sample hundreds of electrodes of different sizes at high sampling rates, but they are very expensive and typically not part of the clinical infrastructure. While technologically superior, they are often not available or practical for clinical use. Thus, it is quite likely that many centers will use microelectrodes with their traditional EEG acquisition systems; it is crucial to understand how this practice will affect data collection and interpretation.

The studies listed above used three different types of microelectrodes: 40 m diameter, nonpenetrating platinum-iridium (Pt-Ir) wire studs (hereafter referred to as “surface microelectrodes”) (Stead et al. 2010); 40 m diameter, loose wires (Pt-Ir) extruded from the end of a depth electrode (“depth microelectrodes” hereafter) (Worrell et al. 2008); and a 96-channel microelectrode array (MEA), with penetrating silicon microelectrodes (5 m wide at the distal ends, platinum-coated on the distal 70 m) (Schevon et al. 2009). One important property used to characterize electrodes is impedance, which is typically reported as a single measurement (e.g. 322 ± 138 KΩ in the MEA (Schevon et al. 2009) or 0.5 to 1 MΩ in depth microelectrodes (Worrell et al. 2008)). However, electrode impedance is, by definition, a frequency-dependent property and therefore cannot be accurately represented by a single

value. With the growing implementation of a tool such as microelectrodes, it is critical to know its behavior and specifications, especially in comparison with the current standard, macroelectrodes. Since the macro- and microelectrodes have similar electrochemical properties, surface area is the primary variable to determine impedance magnitude. The large difference in electrode size results in a large disparity in impedance, which can alter the signal recorded by the system if amplifiers are not designed correctly. This paper demonstrates that while typical clinical amplifiers work very well with macroelectrodes, they can distort low frequency features when used with microelectrodes.

METHODS

We performed a series of experiments to characterize recordings of neural activity using micro- and macroelectrodes. We first characterized the electrodes using electrochemical impedance spectroscopy (EIS), and then built equivalent digital filters to match the electrode and amplifier properties (Fig. 1). Next we generated neural signals using a previously published computational model that mimicked a variety of phenomena (sharp waves, HFOs, multiunits) that are commonly seen in iEEG. We passed the neural signals through the digital filters and examined the extent to which signals were distorted by each electrode and amplifier system. Lastly, we quantified how each acquisition system filtered the signal by measuring features commonly used to analyze EEG data.

Electrode impedance

Unused, clinical-grade micro- and macroelectrodes were tested with EIS using a Gamry Reference 600 Potentiostat (Gamry Instruments, Warminster, PA). Electrodes were submersed in 0.1M phosphate-buffered saline (PBS) with a platinum counter electrode and saturated calomel reference electrode. Each electrode was tested separately by measuring the response to a 25 mV sinusoid at 54 logarithmically-spaced frequencies from 1 Hz to 100 KHz to determine the complex impedance at each frequency, in a manner similar to previously published methods (Lempka et al. 2009). The data for each electrode were fit to circuit parameters with the Gamry Echem Analyst fitter program (installed on a Windows 7 PC), best represented by a resistor in parallel with a combination of Complex Phase Element (CPE) and porous-bounded Warburg impedance (Fig. 1B), which differs from a traditional resistor-capacitor circuit due to the electrode interface (McAdams and Jossinet 1995). EIS data underwent spline interpolation in Matlab (Mathworks Inc., Natick, MA) to be evenly spaced and the complex conjugates were reflected to make a Hermitian transfer function. The value at 0 Hz, which is not tested by the EIS, was set to the value of the resistor R_0 in the equivalent circuit of each electrode (Fig. 1B).

Signal filtering due to electrodes

The “acquired” signal in an EEG acquisition system is the voltage that is recorded by the amplifier. That voltage is not necessarily the same as the signal presented to the recording electrode: the electrode and amplifier form a voltage divider (Fig. 1A). Mathematically, this voltage divider defines the transfer function of this circuit, which characterizes the relationship between the input and output of the system (Nelson et al. 2008). Ideally, the amplifier impedance should be very large compared with the electrode. This assures that the voltage drop across the electrode is small compared to the voltage drop across the amplifier, and therefore that the recorded signal is as close as possible to the original.

In order to determine the transfer functions, the recorded impedances for each electrode were combined with impedance from several different amplifier systems to simulate their response when used with different recording devices. The amplifier impedances were chosen from published values of three commercial systems. The two “clinical” systems have

input resistances of either 50 MΩ or 10 MΩ in parallel with 8 pF. These specific values are from the 40-channel XLTek EMU40 and the 64-channel XLTek NeuroLink IP 64 (Natus Medical, San Carlos, CA). Nearly identical values are found in most EEG systems (e.g. 12 or 50 MΩ (Grass Technologies, West Warwick, RI); 10 MΩ (Cadwell Laboratories, Kennewick, WA); 10, 50 or 100 MΩ (Nicolet, CareFusion Corporation, San Diego, CA)). We also tested a specialized acquisition system that is frequently used for microelectrode recordings (Blackrock, Salt Lake City), which has input impedance of 10 TΩ in parallel with 1 pF.

The original signal was filtered by calculating its Fast Fourier Transform (FFT), then multiplying it by the transfer function in the frequency domain, and then converting the product back to the time domain signal with inverse FFT (Fig. 1C). This filtering was done for every electrode independently for each amplifier system.

Signal filtering due to brain tissue and electrode wires

Brain tissue and wires both act as low-pass filters. Human brain tissue resistivity has a value of 351 Ωcm (Latikka et al. 2001), while the permittivity is variable from 0.09 to 9 F/m (Gabriel et al. 1996), yielding a cutoff frequency somewhere in the range of 5 KHz to 500 KHz (Butson and McIntyre 2005). In order to model the worst-case scenario, we used the lowest cutoff frequency for these parameters, 5 KHz. This filter was applied to the signal before arriving at the electrode. Wire impedance (10 Ω with a stray capacitance of 8 pF/foot of wire) was added to the electrode impedance (Fig 1A).

Input signal

A sample neural signal was generated using a previously published computational model of cortical brain activity (Stacey et al. 2011b; Stacey et al. 2009) in NEURON modeling software (Hines and Carnevale 1997). This signal contained a mixture of potential EEG signals: DC offset, slow activity, sharp waves (150 ms), HFOs (175 Hz), and multiunit action potentials (2 ms). This input waveform contains the full range of frequencies and neural activity typically studied in iEEG. Using this modeled signal allows precise knowledge of the neural activity underlying the signal and is an explicit method to ensure that every electrode receives identical input. Most importantly, it allows direct comparison with the precise, original signal that the electrode tip ‘sees’, which is never known during *in vivo* or *in vitro* experimental measurements.

Feature analysis

After filtering by the electrode and amplifier, the signal was then analyzed using several common quantitative measurements (see Table 1). These features are the basis of many automated algorithms currently in use or under development for analyzing iEEG data. We performed each automated measurement on every simulated recorded signal and the original, raw signal. An example of the original and recorded signals, with their respective amplitudes, is shown in Fig. 1C.

RESULTS

Electrochemical impedance spectroscopy

A total of 106 clinical electrodes and 2 electrodes from an MEA (Blackrock Microsystems, Salt Lake City, UT) were tested. Clinical electrodes were manufactured by either Ad-tech Medical Instrument Corporation (Racine, WI) or PMT Corporation (Chanhassen, MN). Each electrode was measured individually for EIS. As seen in Fig. 2, the macroelectrodes had much lower impedance than the microelectrodes and had very consistent phase response, with the exception of one outlier. The outlier was likely due to a broken wire, an occurrence

that is occasionally seen in clinical macroelectrode recordings, but easily recognized due to the great disparity with its neighbors (such electrodes are typically ignored). Microelectrodes were more varied. Some of the surface microelectrodes had low impedance and were quite similar to the macroelectrodes, while others were several orders of magnitude higher. Their phase response was not consistent. These differences were present even between neighboring electrodes on the same strip. The depth microelectrodes were very similar to the surface microelectrodes, although they were more prone to outliers: two had extremely high impedances and one had a very low impedance. The two MEA electrodes had very different impedances, though these differences were within the same range as the other microelectrodes, and are included within the graph for the depth microelectrodes as hollow circles (Fig. 2C). One striking similarity between all electrodes tested was that the slope of the magnitude in the log-log graphs was nearly identical for all 108 electrodes tested, even the outliers. This slope is dependent on several factors, most notably the electrochemistry of the electrode interface and diffusive effects, which correspond to the exponents in the CPE and Warburg impedances (Fig. 1B). As each of these electrodes contained similar materials and was tested in the same bath, it is not surprising that these electrochemical effects are so similar between electrodes. The primary difference between electrodes was the surface area, which explains the difference between the macro- and microelectrodes. The data in Fig. 2B-C also suggest that there may be a large disparity in effective surface area among the microelectrodes. Further study will be necessary to determine the relationship between surface area and impedance. The summary of the results for 2 frequencies is shown in Table 2.

The EIS data from each electrode were fit to the equivalent circuit model in Fig. 1B. With the exception of the outliers (which behaved like pure capacitors), this model fit to within 5% of the measured data. R_0 was used only for 0 Hz impedance; for all other frequencies the analysis used interpolated impedances from the actual experimental results. The results in Fig. 2 demonstrate several points. First, the spectral response of all intact electrodes is well modeled by CPE + Warburg impedances, and the slope of the magnitudes (in log-log graphs) is remarkably consistent across electrodes. Second, MEA, depth and surface microelectrodes all fall within a similar range of impedances that are much higher than macroelectrodes. Third, unlike macroelectrodes, the microelectrodes have inconsistent phase responses and more variability in magnitude, even on the same electrode grid.

For the remainder of this paper, four examples were chosen from these electrodes: one macroelectrode (green traces), two from the range of surface microelectrodes (red and purple traces), and one depth microelectrode (yellow traces). The results from each of these specific electrodes are shown with the corresponding colors in all subsequent figures.

Filtering effects of tissue and wires are minimal in iEEG

Within clinical circles, there is often much speculation about the role of tissue impedance in filtering iEEG signals. However, previous measurements in monkey brains demonstrated that there is negligible filtering from brain parenchyma, and that signal attenuation is likely due to other physiological factors (Logothetis et al. 2007). Our analysis corroborated this finding: with the 5 KHz low-frequency cutoff, which is the worst-case scenario for tissue filtering, there was negligible filtering on the neural signals (Fig. 3A). Measurement using all analytic features (see next section) showed that the only effect of tissue filtering was a < 5% change in the amplitudes and variance of unit activity (not shown).

The filtering effect of the wire was tested by adding an additional impedance in series with the electrode, simulating a wire from 5 to 500 feet long (40 - 4000 pF). Even at such an extreme value, adding a wire did not have any measureable effect on the signal (data not shown), although noise effects that would be present on such a long wire were not included.

Effect of amplifier impedance

Any distortion (filtering) of the recorded signal is a direct result of the mismatch between electrode and amplifier impedance in the voltage divider (Fig. 1A). This filtering, defined by the transfer function, is expressed using a Bode plot showing the magnitude and phase as a function of frequency (Fig. 3B). The ideal condition is when the transfer function approaches unity (magnitude = 1, phase = 0), meaning the input signal is not attenuated (i.e. not filtered). For this to be true, the amplifier impedance must be very large compared to the electrode. As seen in Fig. 3B, the Bode plot for the 10 TΩ amplifier is unity for all but one of the microelectrodes. The fourth (red) microelectrode will have small amplitude attenuation across all frequencies with no phase distortion. Such is not the case for the 10 or 50 MΩ amplifiers: the signals from macroelectrodes will be unchanged, but signals from microelectrodes will be distorted at low frequencies. The effect is much more pronounced for the 10 MΩ case, in which the transfer function is not unity even beyond 100 Hz. This disparity produces the varied results seen in the later sections.

For comparison, the input resistance of the amplifier was increased until the magnitude of the Bode plot = 1 for all frequencies, as in the 10 TΩ case, for > 50% of the microelectrodes measured. We found that the amplifier impedance had to be greater than 1 GΩ for the majority of microelectrodes to behave similarly to macroelectrodes and not filter the signal. This analysis demonstrates three points: 1) macroelectrodes are well suited for all amplifiers tested; 2) signals will be distorted when recorded by microelectrodes in both clinical systems tested, considerably worse in the 10 MΩ case; and 3) amplifiers should have a minimum input resistance of 1 GΩ in order to acquire comparable signals from macroelectrodes and microelectrodes.

Feature analysis

Acquired signal—Although it is clear from Fig. 3 that it is preferable to record microelectrodes with high-impedance amplifiers, they are not always available in clinical practice. The majority of epilepsy centers currently utilize systems with 10-50 MΩ amplifiers. We therefore used those parameters with the EIS data of the four sample electrodes used in Fig. 2. The simulated recorded signals produced by each electrode are shown in Fig. 4A. The figure demonstrates the acquired signal that would be recorded by each of the 4 electrodes connected to a 10 MΩ amplifier, compared with the original signal (light blue). The same process was used to test the response of each electrode using the 50 MΩ and 10 TΩ amplifiers. With a 50 MΩ amplifier the response was very similar to Fig. 4A, but with slightly less attenuation. The response with a 10 TΩ amplifier was essentially identical to the input signal. After determining what the signals would look like from each electrode, we processed the simulated recorded data with several automated analysis methods.

Amplitude—The original signal has a large DC component (~300 mV), which was strongly filtered by the higher-impedance electrodes. This resulted in large differences in the amplitude of the signal recorded at each electrode. The signal was then detrended and divided by the standard deviation of the baseline (Table 1) to determine whether such signal processing techniques could remove the disparity between amplitudes at different electrodes. Results for each electrode were also normalized to that of the original signal to compare across measurements. As seen in Fig. 4B, all amplitude measurements were strongly affected by electrode impedance. The data recorded on the macroelectrodes were essentially identical to the original signal, while the microelectrode data were highly dependent on impedance, which varied from electrode to electrode.

Cross-covariance and phase—The original signal was covaried with each simulated recorded signal for a window +/- 50 ms during the three sharp wave/HFO events (Fig. 4C). Each cross-covariance was normalized to the peak autocovariance of the original signal. The cross-covariance demonstrates the rhythmic HFOs present in the two later events, one at 175 Hz and the other at 88 Hz. In each case, the signal recorded through the macroelectrode was identical to the original signal. In contrast, there was large amplitude attenuation and phase distortion in all 3 microelectrode recordings.

Power spectral density (PSD) and variance—The PSD and variance were computed over the entire signal. PSD was very similar for frequencies > 100 Hz in all but the highest impedance microelectrodes, but differed considerably below 60 Hz (Fig. 4D). A separate PSD was computed for a 75 ms window during each event (data from the three events were similar, only event #2 is shown, Fig. 4E). The total spectral power for several frequency bands was then computed to show which was most sensitive to impedance. The lowest frequencies were the most affected, especially in the 0-30 Hz band that defines the traditional “Berger bands” of clinical epilepsy. Variance was strongly affected as well. The highest impedance electrode had attenuated band power even at 1000-2000 Hz. These results show that macroelectrode recordings are essentially identical to the original signal, but microelectrodes remove a large portion of the low frequency content that is very dependent on their individual impedance.

Line length—Line length is a simple algorithm used to detect seizures or HFOs, depending on its tuning. It was set to detect HFOs by bandpass filtering the acquired signal from 100-500 Hz and calculating line length in an 85 ms window, as described in (Gardner et al. 2007). There were negligible differences between most of the electrodes, except for decreased amplitude in the electrode with highest impedance (Fig. 4F). Using line length to detect HFOs would work in all electrodes but require a different threshold for the highest-impedance electrode.

Effect of 0 Hz impedance

The above results assumed that the DC (0 Hz) impedance of each electrode was the fitted value of R_0 in Fig. 1B. However, that circuit actually predicts that impedance increases logarithmically as frequency is reduced, going to infinite impedance at 0 Hz. Thus, R_0 may underestimate the true impedance at 0 Hz. It is not straightforward to measure this impedance and compare it with EIS: it represents a non-physiological use of the electrode that is dependent upon irreversible electrochemical reactions (Merrill et al. 2005), which vary greatly depending upon the medium. In order to account for the possibility of even higher impedance at 0 Hz, we retested all of the preceding features assuming the impedance at 0 Hz was a multiple of the resistance in the equivalent circuit. Even with 10000 times higher impedance, the only effect was a DC shift, which affected only the amplitude measurements (not shown). This change did not affect any other measurements, and was present even in the 10 TΩ amplifier. Therefore, the only error this assumption might produce is a modest shift in the DC offset.

Summary: Quantitative measurements in different amplifiers

We measured the features of all 108 electrodes with each amplifier type. A summary of the results is shown in Fig. 5. For amplifiers that are most commonly used with inpatient human iEEG recordings (10 MΩ or 50 MΩ), over half of the microelectrodes produce dramatic changes in DC bias, amplitude, cross-covariance, variance, and spectral power below 60 Hz. Not only were the values smaller in magnitude than the original signal, they are also much more variable (wider quartile bars). In practice, this would result in vastly different results from neighboring electrodes, and might lead to false conclusions.

Features that relied on high frequency content, such as line length and spectral power > 60 Hz, were quite consistent. For over 90% of electrodes with any amplifier, these features in the simulated recorded data were essentially identical to those in the original signal. Macroelectrodes recorded the original signal essentially perfectly in all frequency bands with all amplifiers.

There were some microelectrodes with very high impedance that produced distorted signals over a wide range of frequencies and amplifiers. These included the outliers seen in Fig. 2C as well as several other microelectrodes in 2B. In these electrodes, DC bias and amplitude were attenuated even with a 10 TΩ amplifier. Similarly, they attenuated frequencies up to 2 KHz (e.g. Fig. 4E).

These results lead to several important conclusions. First, clinical amplifiers work exactly as desired with the macroelectrodes, not altering the signals at all in any of the quantitative measures. Second, most microelectrodes record the signals nearly perfectly with the 10 TΩ amplifier (save for tiny DC shifts), lending credence to published results that used similar high impedance systems (Schevon et al. 2009; Stead et al. 2010). Lastly, there is high likelihood of distortion, manifesting as errors in several signal features, when microelectrodes are used with typical clinical systems (impedance <= 50 MΩ). Based upon this sample of 96 microelectrodes,, an amplifier needs to have input impedance of at least 1 GΩ, or 100 times greater than the amplifiers commonly sold in clinical systems, to assure that > 50% of the microelectrodes will correctly record the signal.

DISCUSSION

Strengths and limitations of testing method

Our method of measuring EIS and using it as a transfer function to filter the signal has some important strengths and limitations. We decided on this explicit method in order to control for two key variables: we had to assure that each electrode received the identical input; and each electrode had to be tested with multiple amplifiers, including some theoretical specifications (1GΩ). Direct testing of signals in solution would have introduced unavoidable errors: electrode recordings are highly dependent on distance to the source and the ionic content of the media, and there would be fluctuations between measurements on different amplifiers. EIS is the most controlled method available to test impedance, and the mathematical filtering thereafter has a strong foundation in basic engineering principles. The EIS values were very consistent in all electrodes, even in the outliers. This provided straightforward interpolation and good resolution in the frequency domain that was suitable for data sampled at 40 KHz. The EIS magnitudes (Fig. 2) also demonstrate remarkable similarity between electrodes: the slopes are all nearly identical in log-log space, suggesting that they could be predicted with many fewer measurements.

There are several important limitations to this implementation. First, as described above there was no EIS measurement at 0 Hz and we had to make an assumption for that one data point. We tested several values and demonstrated that our assumption is likely valid within a small DC offset in the processed data. Second, the transfer functions rely upon published impedance data for the three amplifiers. Any variation in those parameters in the actual system will change the response accordingly. Third, our implementation did not include the effects of noise. Larger impedance produces higher levels of thermal noise, and neural signals have frequency-dependent “1/f” noise. Both of these noise sources will have complex effects on these electrodes, although they can be minimized with careful engineering (Lempka et al. 2011). Despite these limitations, we feel this method is a good representation of the signal recorded by each electrode and amplifier system.

Choice of acquisition systems for use with microelectrodes

Microelectrodes have much higher and more variable impedance than macroelectrodes. Both of these disparities are exacerbated by having low impedance amplifiers. The variability among microelectrodes, even on the same grid, is especially concerning as it could easily lead to erroneous interpretations about the localization of electrophysiological phenomena. These results highlight the need to consider the electronic specifications of the EEG system when using microelectrodes. This is not to say the amplifiers chosen for this study are inferior to other systems—they were designed for macroelectrodes and work perfectly well with them; they only have errors when connected to the newer microelectrodes.

Clearly, the ideal case is to have amplifiers with much higher input impedance, and electrodes with more consistent impedances. There are high-impedance systems available: the Blackrock (Salt Lake City) amplifier is approved for clinical use, and there are other clinical systems with high input impedance (e.g. SynAmps RT (10 GΩ) Compumedics Neuroscan, Charlotte, NC). However, the majority of epilepsy centers do not use these specialized systems in clinical practice: 10 MΩ amplifiers work perfectly well with macroelectrodes so there has been little incentive to change. Until high-impedance clinical amplifiers are more readily available, the options for recording with microelectrodes are either to acquire specialized equipment or to continue using the preexisting, lower-impedance clinical systems. In the latter case, the data in Fig. 5 can serve as a guideline for comparing data from different electrode types: measurements of amplitude, variance, phase and power spectra under 60 Hz are attenuated and variable with microelectrodes, while higher frequency content is minimally affected. It is therefore crucial to take great care drawing conclusions about the response at different electrodes, to assure the differences are not simply due to impedance effects.

CONCLUSION

We have shown that there is significant variability in the impedance of microelectrodes used for intracranial EEG, even among electrodes on the same device. Impedances from surface microelectrodes, depth microelectrodes, and the MEA have magnitudes that are around 100 times higher than that of typical macroelectrodes, which makes them too high to use reliably with many clinical iEEG amplifiers. This imbalance with the amplifier causes distortion of the EEG signal, which can make the same physiological data look differently at neighboring electrodes. To avoid this, amplifiers with impedance of at least 1 GΩ should be used, which unfortunately is beyond the range of most clinical systems. If such amplifiers are not available, special care must be taken in analyzing and comparing data from microelectrodes to address the effects of varied impedance. In light of these data, it is our hope that electrode manufacturers improve the variability of microelectrode impedances, and EEG manufacturers provide higher impedance amplifiers that are more appropriate for these new electrodes.

Acknowledgments

The authors would like to thank P. Walker for his helpful discussions. WS planned, carried out the analysis and wrote the article. SK, PP, and BG acquired data. CB planned and assisted writing the article.

This work was supported by the National Institutes of Health [K08NS069783 to W.S.]

SOURCES CITED

Butson CR, McIntyre CC. Tissue and electrode capacitance reduce neural activation volumes during deep brain stimulation. Clin Neurophysiol. 2005; 116:2490–2500. [PubMed: 16125463]

Cimatti Z, Schwartz DP, Bourdain F, Meunier S, Bleton JP, Vidailhet M, Renault B, Garnero L. Time-frequency analysis reveals decreased high-frequency oscillations in writer's cramp. Brain. 2007; 130:198–205. [PubMed: 17003068]

Gabriel S, Lau RW, Gabriel C. The dielectric properties of biological tissues: II. Measurements in the frequency range 10 Hz to 20 GHz. Phys Med Biol. 1996; 41:2251–2269. [PubMed: 8938025]

Gardner AB, Worrell GA, Marsh E, Dlugos D, Litt B. Human and automated detection of high-frequency oscillations in clinical intracranial EEG recordings. Clin Neurophysiol. 2007; 118:1134–1143. [PubMed: 17382583]

Hines ML, Carnevale NT. The NEURON simulation environment. Neural Comput. 1997; 9:1179–1209. [PubMed: 9248061]

Latikka J, Kuurne T, Eskola H. Conductivity of living intracranial tissues. Physics in Medicine and Biology. 2001; 46:1611–1616. [PubMed: 11419622]

Le Van Quyen M, Staba R, Bragin A, Dickson C, Valderrama M, Fried I, Engel J. Large-scale microelectrode recordings of high-frequency gamma oscillations in human cortex during sleep. J Neurosci. 2010; 30:7770–7782. [PubMed: 20534826]

Lempka SF, Johnson MD, Moffitt MA, Otto KJ, Kipke DR, McIntyre CC. Theoretical analysis of intracortical microelectrode recordings. J Neural Eng. 2011; 8:045006. [PubMed: 21775783]

Lempka SF, Miocinovic S, Johnson MD, Vitek JL, McIntyre CC. In vivo impedance spectroscopy of deep brain stimulation electrodes. J Neural Eng. 2009; 6:046001. [PubMed: 19494421]

Logothetis NK, Kayser C, Oeltermann A. In vivo measurement of cortical impedance spectrum in monkeys: implications for signal propagation. Neuron. 2007; 55:809–823. [PubMed: 17785187]

McAdams ET, Jossinet J. Tissue impedance: a historical overview. Physiol Meas. 1995; 16:A1–13. [PubMed: 8528108]

Merrill DR, Bikson M, Jefferys JG. Electrical stimulation of excitable tissue: design of efficacious and safe protocols. Journal of neuroscience methods. 2005; 141:171–198. [PubMed: 15661300]

Nelson MJ, Pouget P, Nilsen EA, Patten CD, Schall JD. Review of signal distortion through metal microelectrode recording circuits and filters. Journal of neuroscience methods. 2008; 169:141–157. [PubMed: 18242715]

Ritaccio A, Brunner P, Cervenka MC, Crone N, Guger C, Leuthardt E, Oostenveld R, Stacey W, Schalk G. Proceedings of the first international workshop on advances in electrocorticography. Epilepsy Behav. 2010; 19:204–215. [PubMed: 20889384]

Schevon CA, Trevelyan AJ, Schroeder CE, Goodman RR, McKhann G Jr. Emerson RG. Spatial characterization of interictal high frequency oscillations in epileptic neocortex. Brain. 2009; 132:3047–3059. [PubMed: 19745024]

Stacey W, Le Van Quyen M, Mormann F, Schulze-Bonhage A. What is the present-day EEG evidence for a preictal state? Epilepsy Res. 2011a; 97:243–251. [PubMed: 21885253]

Stacey WC, Krieger A, Litt B. Network recruitment to coherent oscillations in a hippocampal computer model. Journal of neurophysiology. 2011b; 105:1464–1481. [PubMed: 21273309]

Stacey WC, Lazarewicz MT, Litt B. Synaptic Noise and Physiological Coupling Generate High Frequency Oscillations in a Hippocampal Computational Model. Journal of neurophysiology. 2009; 102:2342–2357. [PubMed: 19657077]

Stead M, Bower M, Brinkmann BH, Lee K, Marsh WR, Meyer FB, Litt B, Van Gompel J, Worrell GA. Microseizures and the spatiotemporal scales of human partial epilepsy. Brain. 2010

Worrell GA, Gardner AB, Stead SM, Hu S, Goerss S, Cascino GJ, Meyer FB, Marsh R, Litt B. High-frequency oscillations in human temporal lobe: simultaneous microwire and clinical macroelectrode recordings. Brain. 2008; 131:928–937. [PubMed: 18263625]

Worrell GA, Parish L, Cranstoun SD, Jonas R, Baltuch G, Litt B. High-frequency oscillations and seizure generation in neocortical epilepsy. Brain. 2004; 127:1496–1506. [PubMed: 15155522]

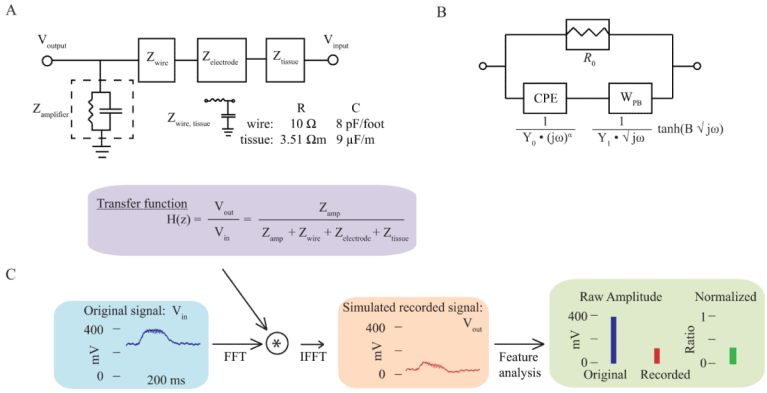

Figure 1. Methods

A: The ratio V_{output}/V_{input} is determined by a voltage divider circuit. This ratio forms the transfer function "H(z)" of the recording system, which describes how much the original signal is distorted at the recording site (purple box). Minimal distortion will occur when $Z_{amp} >> Z_{wire} + Z_{electrode} + Z_{tissue}$ (Z: complex impedance; H(z): discrete time z-transform). The wire, amplifier, and brain tissue impedances are all low-pass parallel RC circuits. The wire and tissue parameters are as shown. B: Equivalent circuit model that best fit the EIS data contained a resistance (R_0) in parallel with a Constant Phase Element (CPE) and porous-bounded Warburg impedance (W_{PB}). The equation fit (varying R_0, Y_0, Y_1, and B) was used to calculate R_0 for the 0 Hz impedance. C: A gold-standard neural signal was generated (blue box). It was transformed to the frequency domain, multiplied by the transfer function, then transformed back to the time domain to create the simulated recorded signal (orange box). Finally, the simulated data were analyzed with various quantitative measurements such as amplitude compared to the original raw signal (green). In this case, the simulated amplitude is about 30% of the original.

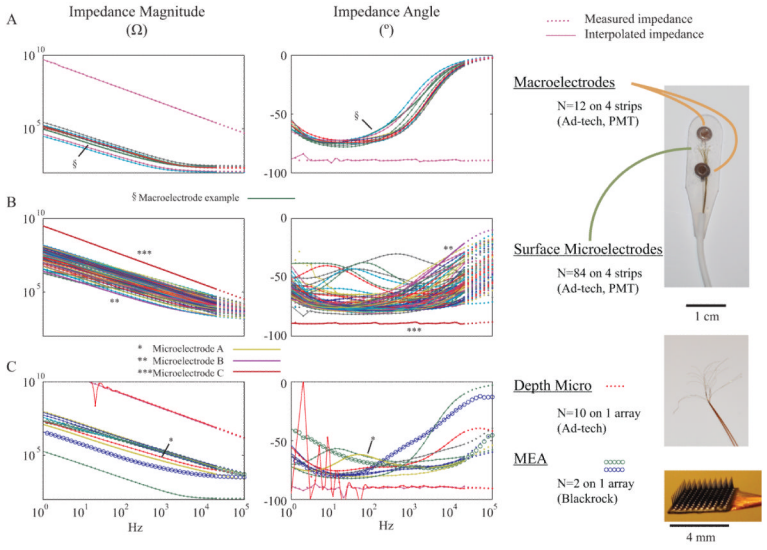

Figure 2. EIS

A: EIS for the 12 macroelectrodes. Magnitude (left) and phase angle (right) are consistent except for one obvious outlier, which was excluded from further analysis. §-macroelectrode used for analysis in later figures (green line). Dotted line: measured values from EIS. Solid line: interpolated values used to produce H(z) at regular frequencies. B,C: Magnitude (left) and phase (right) of surface and depth microelectrodes, respectively. Data from 2 MEA are shown in C with hollow circles. *, **, ***: three electrodes (yellow, purple, red) used in later figures, representing the full range of microelectrodes. Photographs: A “hybrid” grid containing 2 macroelectrodes and 8 microelectrodes (top), the depth microelectrode array (middle) and an MEA (bottom, P. House, used with permission).

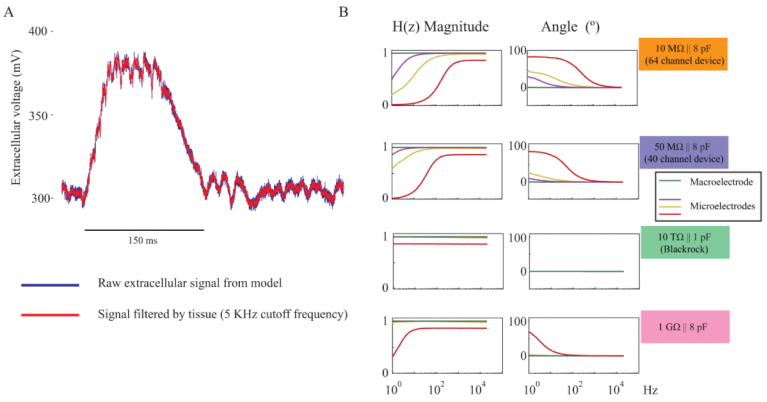

Figure 3. Data Filtering

A: Original signal (blue) overlayed with tissue-filtered data (red). There is very subtle filtering of high frequencies, but neural activity is essentially unchanged. B: Transfer functions for the 4 electrode examples from Fig. 2. The EIS data from each electrode were combined with the specifications of 4 amplifiers: two clinical systems (10 and 50 MΩ), a specialized system (10 TΩ), and a theoretical device (1 GΩ) that would work well with all but the worst microelectrode. The clinical systems, with 10 and 50 MΩ input resistance, have non-ideal transfer functions at low frequencies, which distorts the signals. The 10 TΩ amplifier has no distortion except for a constant offset in the worst electrode. Results for a theoretical 1 GΩ device, which would have an ideal response for nearly all microelectrodes, are also shown (bottom).

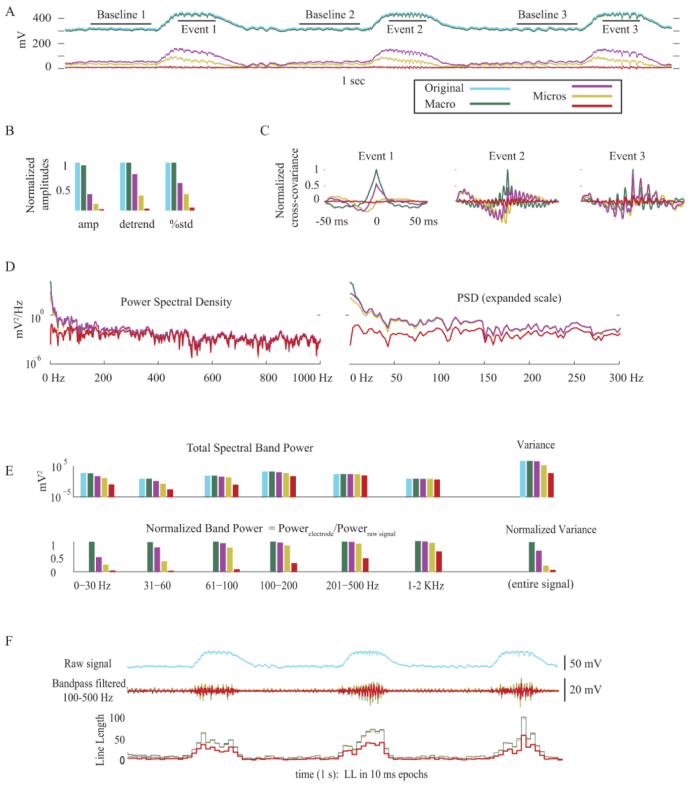

Figure 4. Data analysis amplitude and cross-covariance

A: Acquired signals. The original signal (light blue) is reproduced almost perfectly by the macroelectrode (green), with only a slight DC offset. The three microelectrodes remove most of the low frequency content and are quite variable in appearance. The epochs corresponding to the three sharp wave “events” and their preceding “baselines” are indicated. On this and all further graphs, the colors correspond to the 4 marked electrodes in Fig. 2. B: Event amplitudes demonstrate a strong dependence on electrode impedance, even when detrended or normalized by baseline variance. C: Cross-covariance phase and amplitude are very dependent on impedance. The macroelectrode data is identical to that of the original signal. The differences in the three events are due to the HFOs present in each. D: PSD of the entire signal shows impedance-dependent loss of low frequencies. E: Integrated PSD of the second event over the indicated frequency bands shows that low frequency power is variable but higher frequencies are less affected. Variance also differs greatly among the microelectrodes (right). Top: band power in log scale. Bottom: band power normalized to the value from original signal. F: Acquired signal (top) is bandpass filtered (middle) to produce the line length (bottom). The only significant difference is a lower threshold in the red electrode.

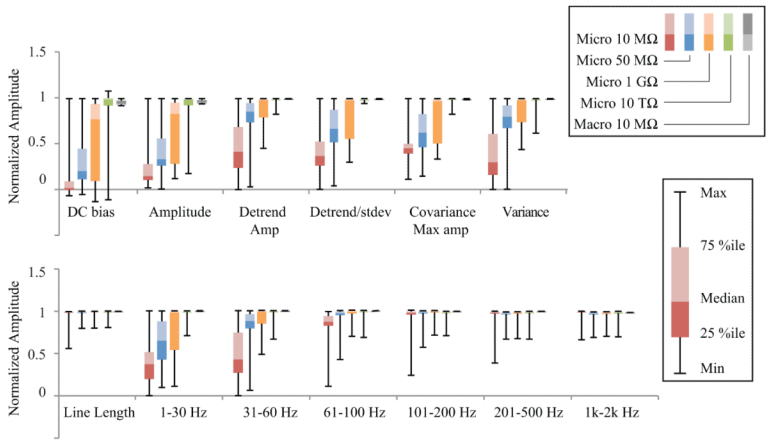

Figure 5.

Feature summary Data from all electrodes (96 microelectrodes, 11 macroelectrodes) with each of the four amplifier types are summarized with box plots (median, quartiles, and range). Each measurement was normalized to the value produced by the original signal. Data for the macroelectrodes are shown just for the 10 MΩ amplifier, as they were uniformly identical to the original signal (far right of each measurement). For the microelectrodes, the two depth outliers seen in Fig. 2C were omitted from the range calculation (but not median and quartiles), as they were 0 for all measurements. These results show that recording with microelectrodes on low impedance amplifiers distorts many features of the EEG signals in over 50% of the electrodes: DC bias, all amplitude measures, peak cross-covariance, variance and spectral power under 60 Hz. The responses were highly dependent on the amplifier impedance. In contrast, line length and spectral power > 60 Hz were quite uniform. The 10 TΩ amplifier produced a signal nearly identical to the original in all measurements, except for loss of DC content with the highest impedance electrodes. A 1 GΩ amplifier had good fidelity for most of the electrodes, but there was still some variability in up to 50% of them.

Table 1

Measurement methods

Measurement	Method
DC Bias	$1/3\sum_{i=1}^{3}\overline{V_{baseline\ i}}$ (baseline: 125 ms window 25 ms before event) i=1
Event Amplitude	$1/3\sum_{i=1}^{3}\overline{V_{event\ i}}$ (event: 75 ms window during sharp wave) / / j event i i=1
Detrended amplitude	$1/3\sum_{i=1}^{3}\overline{V_{event\ i}-V_{baseline\ i}}$
Amplitude/stdev	$1/3\sum_{i=1}^{3}\left(\overline{V_{event\ i}-baseline\ i}\right)/stdev\left(V_{baseline\ i}\right)$
Covariance (xcov)	Normalized cross covariance (original:simulated recorded data)
Power Spectral Density	Welch's PSD of detrended signal, window=3000 samples, overlap=100 samples
Event Spectral Band Power	Integral of PSD of between indicated frequencies
Variance	Variance of entire recorded signal
Line length	10 ms epoch of (100-500 Hz) simulated recorded data as in (Gardner et al. 2007)
Normalization	Me asurement$_{\text{analyzed data}}$ / Measurement$_{\text{original signal}}$

Each of these methods was performed on the simulated recorded data from every electrode. Location of baselinei and eventi are shown in Fig. 4. Solid bar: mean of entire window. Stdev: standard deviation. Where possible, each measurement was normalized to the value produced by analysis of the original, raw signal (Fig. 5).

Table 2

Summary of Electrochemical Impedance Spectroscopy

Electrode (N)	|Impedance| @ 32 Hz	|Impedance| @ 100 Hz
Macro (12)	8045 ± 1725 Ω (1870 Ω – 159 MΩ)	3135 ± 635 Ω (740 – 50.4 MΩ)
Surface μ (84)	2.4 MΩ ± 1.4 MΩ (148 kΩ – 100 MΩ)	889 kΩ ± 515 kΩ (56.2 kΩ – 31.7 MΩ)
Depth (μ (10)	2.5 MΩ ± 1.7 MΩ (8110 Ω – 4.9 GQ)	1 MΩ ± 5.1 kΩ (2790 Ω – 1.5 GQ)
MEA (2)	[180 kΩ, 2.65 MΩ]	[64 kΩ, 1.1 MΩ]

The impedance magnitude at two frequencies for each electrode type. Data shown are median +/- the 25th percentile, with the full range in parentheses. Values for the two MEA electrodes are listed in square brackets.